# Longwave Scattering Effects on Fluxes in Broken Cloud Fields

*E. E. Takara and R. G. Ellingson*
*Department of Meteorology*
*University of Maryland at College Park*
*College Park, Maryland*

The importance of clouds in the radiative energy balance is well known. Since broken cloud fields are prevalent, both the geometry and optical properties of clouds are important parameters. The flat black plate approximation, used by general circulation models for clouds in the longwave, neglects both cloud geometry and optical properties. The error in neglecting geometry has been shown in many works (Ellingson 1982; Harshvardhan and Weinman 1982; Killen and Ellingson 1994).

The single scattering albedo ($\tilde{\omega}_0$ of clouds in the shortwave is 0.99 or higher (Hu and Stamnes 1993). Therefore, most of the previous works on the effects of cloud scattering have been in the shortwave (Welch and Wielicke 1984; Evans 1993; Breon 1992). But the longwave ($\tilde{\omega}_0$) can be as high as 0.75 (Hu and Stamnes 1993), so longwave scattering effects can be significant. In this work, the fluxes above and below a single cloud layer are presented, along with the errors in assuming flat black plate clouds or black clouds.

The predicted fluxes are the averaged results of analyses of several fields with the same cloud amount. Each analysis is in two parts: generating a cloud field and then calculating the fluxes. The cloud size distribution of Cahalan and Joseph (1989) was adapted:

$$\frac{n(a)}{n(a_0)} = \left[\frac{a}{a_0}\right]^{-1.5} \qquad (1)$$

The exponent, -1.5, was changed from the original -1.6 in order to simplify the calculation. The clouds were in five cloud size groups (1, 4, 9, 16, and 25 times $a_0$ non-overlapping and randomly distributed in space. Figure 1 shows the top/bottom view of a cuboidal field; N = 0.15. The fluxes were computed using the Monte Carlo method. To simulate an infinite cloud field, cyclical/specular horizontal boundaries were assumed.

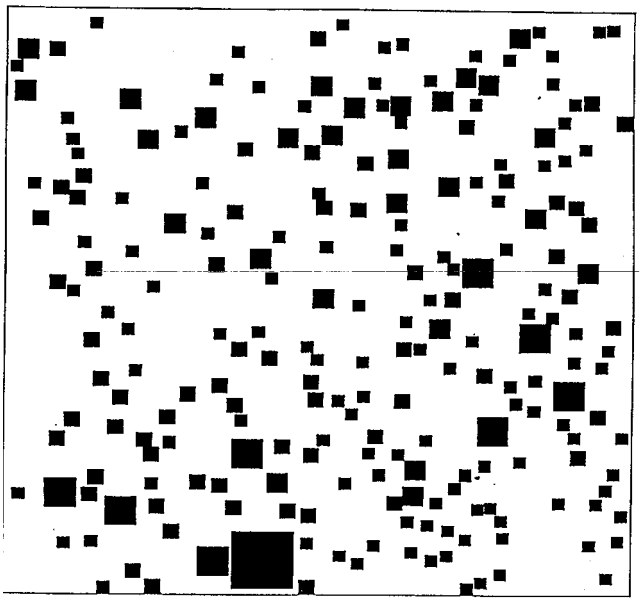

**Figure 1**. Random cloud field with 15% cloud cover.

Four assumptions were made in order to emphasize the effect of scattering in the atmospheric window as well as simplifying the calculation. First, the gaseous absorption is neglected. Second, the cloud optical properties are constant over the 800 $cm^{-1}$ to 1200 $cm^{-1}$ window region. Third, the cloud field is a single layer with clouds of the same base height, aspect ratio, and either cuboidal or cylindrical. Last, the optical properties and temperature were assumed to be constant over all clouds in the field.
The cloud temperatures were set at 15°C, −10°C, and −50°C, corresponding to low, middle, and high clouds at 0, 4, and 10 km, respectively. Another measure of cloud height is to normalize the integral, over the window region, of the Planck function at the cloud temperature with the same integral at the surface temperature (27°C).

$$\xi = \frac{\int_{8.33\ \mu m}^{12.5\ \mu m} E_{\lambda,\,b}^{cloud}(10\ \mu m)}{\int_{8.33\ \mu m}^{12.5\ \mu m} E_{\lambda,\,b}^{ground}(10\ \mu m)} \qquad (2)$$

At the cloud temperatures considered, the $\xi$ are 0.822, 0.516, and 0.200.

The above cloud upward flux and the below cloud downward flux were computed for cuboidal and cylindrical cloud fields of various aspect ratio ($\alpha$), base cloud fraction (N), smallest cloud horizontal optical thickness (L), and single scattering albedo ($\omega_0$). For a given N, results were averaged until the deviation in the cloud absorption ratio was under 2% for a minimum of five fields. Figure 2 illustrates the geometry and relevant variables.

The upward and downward fluxes for cuboidal and cylindrical fields are shown in Figures 3a,b,c,d and 4a,b,c,d. The fluxes at N=1 were computed using the independent pixel approximation. The fluxes for black clouds are not shown because the fluxes for absorbing clouds ($\omega_0$ = 0) with L=100 are nearly identical. There is little variation between the fluxes for L=100 and L=10, or between cylindrical and cuboidal cloud fields. The similarity between cylindrical and cuboidal clouds is not too surprising. Both have constant vertical cross section and are indistinguishable when seen from large horizontal distances.

In general, the fluxes are grouped by aspect ratio $\alpha$ for small cloud amounts N. As cloud amounts increase, individual clouds become indistinct. So, at large N, the fluxes are grouped by $\omega_0$. The variation in the above cloud upward flux with $\omega_0$ for large N decreases with elevation. The below cloud flux variation increases

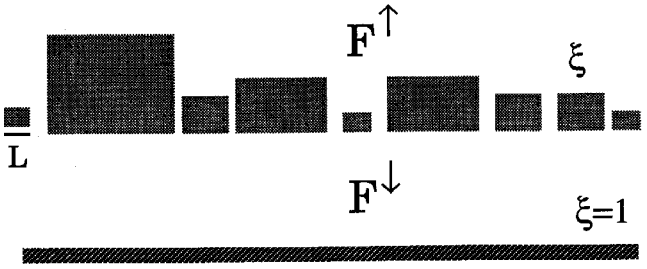


**Figure 2**. Cloud field parameters and vertical geometry.

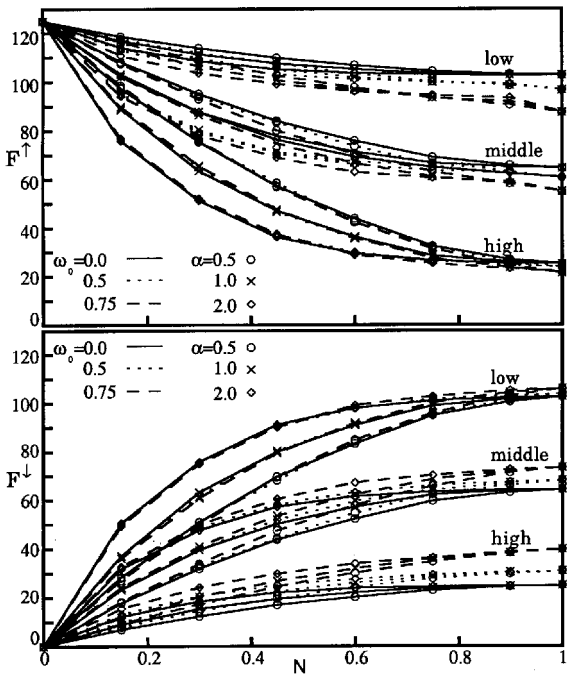


**Figure 3a,b**. Fluxes (W/m$^2$) for cuboidal clouds; L=100.

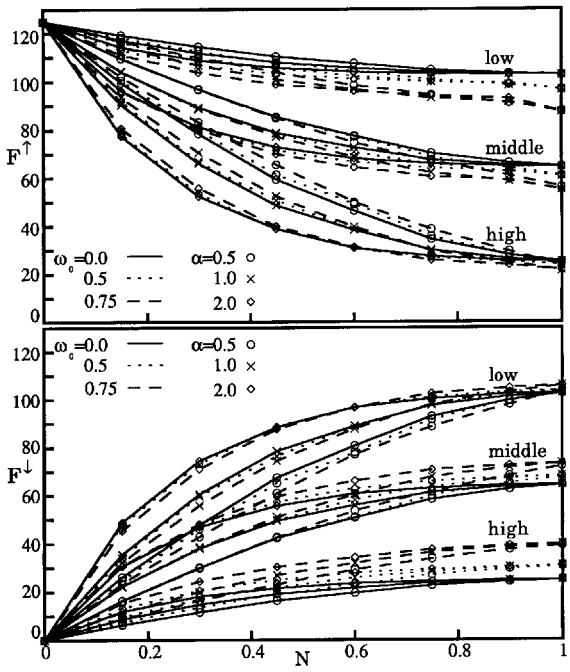


**Figure 3c,d**. Fluxes (W/m$^2$) for cuboidal clouds; L=10.

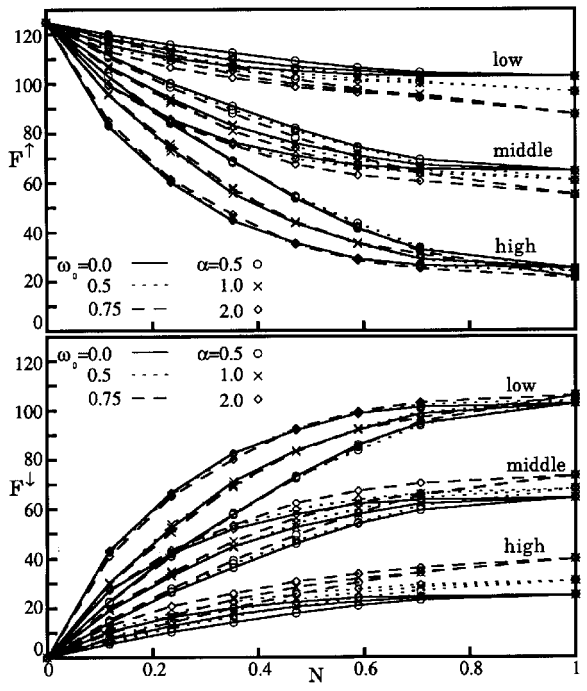


**Figure 4a,b**. Fluxes ($W/m^2$) for cylindrical clouds; L=100.

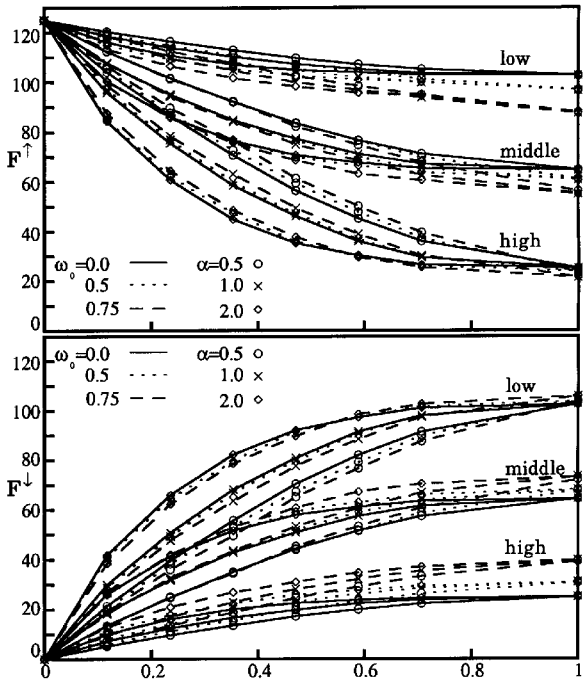


**Figure 4c,d**. Fluxes ($W/m^2$) for cylindrical clouds; L=10.

magnitude of the variation is about the same; but on a percentage basis, highest for high cloud $\Psi_{down}$.

In the flat black cloud approximation, the cloud field is replaced by a field of black plates with the same N. In the geometric black cloud approximation, the cloud field geometry remains the same, but the individual clouds become black. Fluxes computed using the flat black plate and geometric black cloud approximations were compared with the computed fluxes. The absolute and percentage flux errors are

$$\delta F = F^{approx} - F \quad ; \quad \% F = 100 \; X \left[ \frac{\delta F}{F} \right] \qquad (3)$$

The flat black plate maximum absolute and percentage errors for upward and downward fluxes are shown in Figure 5a,b,c,d. The absolute and percentage errors in the upward flux are largest for high clouds. These errors are solely due to neglecting geometry, scattering does not have a significant effect on high cloud upward flux. The error peaks at water vapor, reduces the scattering effects N = 0.3, and then decreases. This peak is characteristic of flat plate approximations. Note that the error for the tall clouds ($\alpha = 2$) may not be important since high clouds tend to have low aspect ratio. The downward flux absolute

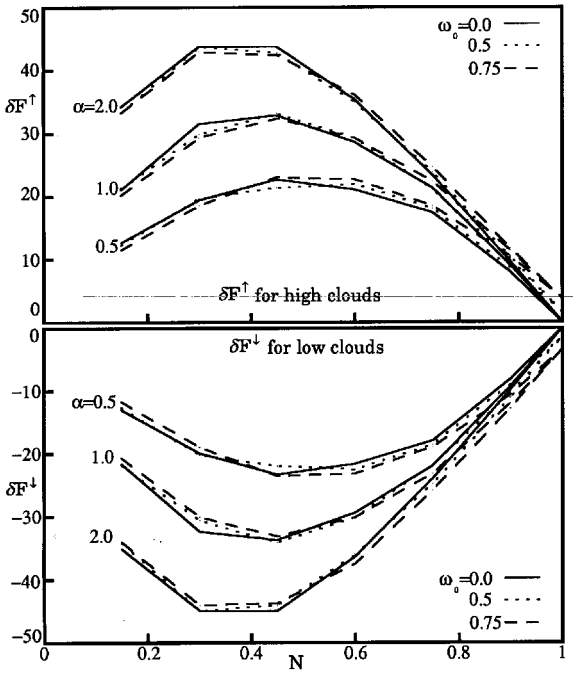


**Figure 5a,b**. Maximum absolute flux error ($W/m^2$) for the flat black plate approximation.

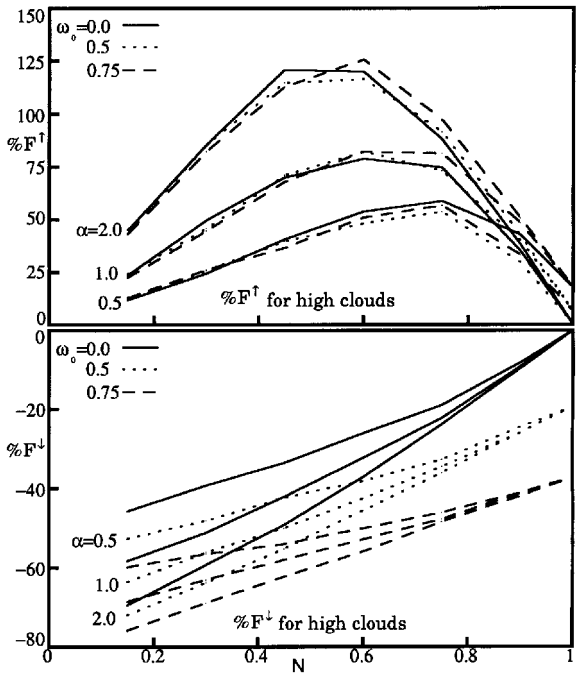


**Figure 5c,d**. Maximum percentage flux error for the flat black plate approximation.

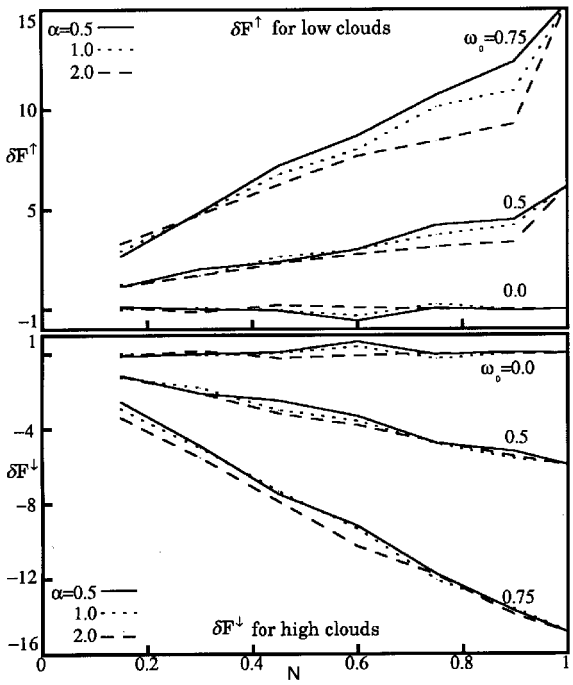


**Figure 6a,b**. Maximum absolute flux error ($W/m^2$) for the geometric black cloud approximation.

error is largest for low clouds and decreases with elevation. The range of the percentage error for the downward fluxes is relatively constant (-80%) for all cloud elevations, high clouds were chosen because they show the most variation with $\omega_0$.

The geometric black cloud maximum absolute and percentage errors for upward and downward fluxes are shown in Figure 6a,b,c,d. The absolute error in the upward flux is much smaller than the flat black error and has more linear behavior, steadily increasing to a maximum at N = 1. The upward flux percentage error has roughly the same range for all cloud heights and is much less than the percentage error from the flat black plate approximation. The maximum downward flux errors are for high clouds; this is where scattering is most important. While the error is large, it is still smaller than the error from the flat black plate approximation.

The results show that scattering can have a significant effect on the fluxes. This is seen in low cloud upward flux and high cloud downward flux. To attain high percentage accuracy, scattering must not be neglected. The addition of absorbing gases, especially water vapor, will reduce the scattering effects presented, with the additional complication that water vapor amounts are dependent on latitude.

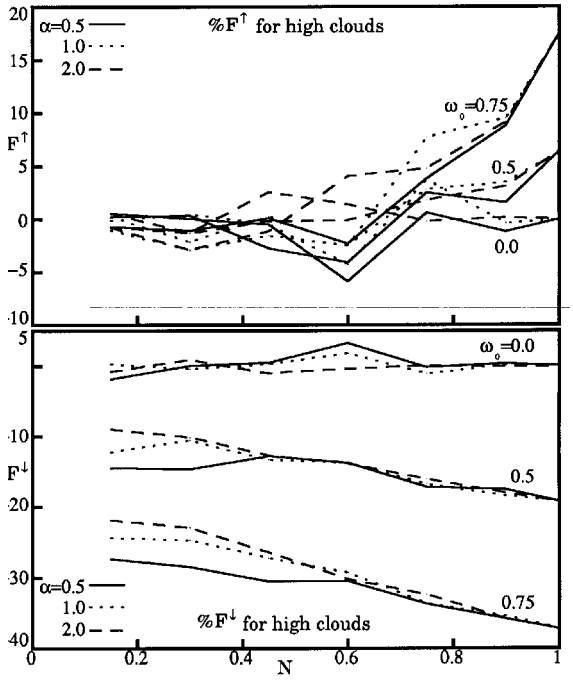


**Figure 6c,d**. Maximum percentage flux error for the geometric black cloud approximation.

## References

Breon, F. M. 1992. Reflectance of broken cloud fields: Simulation and parameterization, *J. Atmos. Sci.*, **49**, 1221-1232.

Cahalan, R. F., and J. H. Joseph. 1989. Fractal statistics of cloud fields, *Mon. Wea. Rev.*, **117**, 261-272.

Ellingson, R. G. 1982. On the effects of cumulus dimensions on longwave irradiance and heating rates, *J. Atmos. Sci.*, **39**, 886-896.

Evans, K. F. 1993. Two-dimensional radiative transfer in cloudy atmospheres. Part I: The spherical harmonic spatial grid method, *J. Atmos. Sci.*, **50**, 3111-3124.

Harshvardhan, J. A., and R. G. Weinman. 1982. Infrared radiative transfer through a regular array of cuboidal clouds, *J. Atmos. Sci.*, **39**, 431-439.

Hu, Y. X., and K. Stamnes. 1993. An accurate parameterization of the radiative properties of water clouds suitable for use in climate models, *J. Clim.*, **6**, 728-742.

Killen, R. M., and R. G. Ellingson. 1994. The effect of shape and spatial distribution of cumulus clouds on longwave irradiance, *J. Atmos Sci.*, **51**, 2123-2136.

Welch, R. M., and B. A. Wielicke. 1984. Stratocumulus cloud field reflected fluxes: The effect of cloud shape, *J. Atmos. Sci.*, **41**, 3085-3103.